Trial wave functions with long-range Coulomb correlations for two-dimensional *N*-electron systems in high magnetic fields

Constantine Yannouleas and Uzi Landman
School of Physics, Georgia Institute of Technology, Atlanta, Georgia 30332-0430
(Received 3 June 2002; published 20 September 2002)

A new class of analytic wave functions is derived for two dimensional *N*-electron ($2 \leqslant N < \infty$) systems in high magnetic fields. These functions are constructed through breaking (at the Hartree-Fock level) and subsequent restoration (via post-Hartree-Fock methods) of the circular symmetry. They are suitable for describing long-range Coulomb correlations, while the Laughlin and composite-fermion functions describe Jastrow correlations associated with a short-range repulsion. Underlying our approach is a collectively-rotating-electron-molecule picture, yielding for all *N* an oscillatory radial electron density that extends throughout the system.

DOI: 10.1103/PhysRevB.66.115315 PACS number(s): 73.21.La, 73.43.−f, 73.22.Gk

I. INTRODUCTION

Two-dimensional (2D) few-electron systems in strong magnetic fields have been the focus of extensive theoretical investigations in the last 20 years.[1–14] Many of these studies have used the Jastrow-Laughlin[2] (JL) and composite-fermion[3] (CF) wave functions, where the dynamics of electrons in extended fractional quantum Hall (FQH) systems is governed by the so-called Jastrow correlations. It was shown[15] that the JL functions are exact eigenstates of the *N*-electron problem under high magnetic fields for a special short-range interparticle repulsion. However, based on close-to-unity overlaps with exact numerical solutions[1,5–11] of the Coulomb problem for few-electron systems (with $N \leqslant 8$), it is believed[2–4,15] that the JL/CF functions should not differ significantly from the exact Coulombic solutions.

Recent experiments[16] on electron tunneling into the edges of a FQH system have found a current-voltage power-law behavior $I \propto V^{\alpha}$, with values for the exponent α that are in conflict with the universal prediction $\alpha = 1/\nu$ derived from Jastrow correlations. These findings motivated[17,18] detailed exact diagonalization studies of FQH systems at the filling factor $\nu = 1/3$ with up to $N = 12$ electrons. These latest studies revealed that the long-range Coulomb correlations lead to the formation of stripe-like oscillations in the radial electron densities (ED's) which are responsible[17] for the observed unexpected behavior of the current-voltage power law. Most importantly, the JL functions fail[18] to capture these ED oscillations, *in spite of having overlaps with the exact wave functions that are very close to unity*.

For the *N*-electron problem in strong magnetic fields and in the disk geometry (case of quantum dots, QD's), we use in this paper a *microscopic* many-body approach to derive analytic wave functions that capture the long-range correlations of the Coulomb repulsion. To obtain analytic results, we specifically consider the limit when the confining potential can be neglected compared to the confinement induced by the magnetic field.

Underlying our approach is a physical picture of a collectively rotating electron molecule (REM) and the synthesis of the states of the system consists of two steps: First the breaking of the rotational symmetry at the level of the single-determinantal *unrestricted* Hartree-Fock (UHF) approximation yields states representing electron molecules (EM's, or finite crystallites). Subsequently the rotation of the electron molecule is described through restoration of the circular symmetry via post Hartree-Fock methods, and in particular projection techniques.[19] Naturally, the restoration of symmetry goes beyond the mean-field and yields multideterminantal wave functions. In contrast to the JL/CF functions, our analytic functions (applicable for any *N* and fractional filling) yield oscillatory radial ED's in agreement with the exact solutions of the *N*-electron Coulombic system (see below).

II. METHOD AND TRIAL WAVE FUNCTIONS

In general, the symmetry-broken UHF orbitals are determined numerically.[13,14,20,21] However, in the case of an infinite 2D electron gas in strong magnetic fields, it has been found[22] that such UHF orbitals can be approximated by analytic Gaussian functions centered at different positions $Z_j \equiv X_j + \imath Y_j$ and forming an hexagonal Wigner crystal (each Gaussian representing a localized electron). Such displaced Gaussians are written as (here and in the following $\imath \equiv \sqrt{-1}$)

$$u(z, Z_j) = (1/\sqrt{\pi}) \exp[-|z - Z_j|^2/2] \exp[-\imath(xY_j + yX_j)], \tag{1}$$

where the phase factor is due to the gauge invariance. $z \equiv x - \imath y$, and all lengths are in dimensionless units of $l_B\sqrt{2}$ with the magnetic length being $l_B = \sqrt{\hbar c/eB}$.

In the case of a Coulombic finite *N*-electron system, it has been found[12,13] that the UHF orbitals arrange themselves in concentric rings forming EM's (referred to also as Wigner molecules, WM's).[23] The UHF results for the ring arrangements are in agreement with the molecular structures obtained via conditional probability distributions (CPD's) which can be extracted from exact numerical wave functions,[10,11,24] as well as with those obtained[25] for the equilibrium configurations of classical point charges in a 2D harmonic trap.[26]

For an *N*-particle system, the electrons are situated at the apexes of *r* concentric regular polygons. The ensuing multiring structure is denoted by $(n_1, n_2, \ldots, n_r)$ with $\Sigma_{q=1}^{r} n_q = N$. The position of the jth electron on the qth ring is given by

$$Z_j^q = \tilde{Z}_q \exp[\imath 2\pi(1-j)/n_q], \quad 1 \leqslant j \leqslant n_q . \tag{2}$$

We expand now the displaced Gaussian [Eq. (1)] over the Darwin-Fock single-particle states. Due to the high magnetic field, only the single-particle states

$$\psi_l(z) = \frac{z^l}{\sqrt{\pi l!}} \exp(-zz^*/2) \tag{3}$$

of the lowest Landau level are needed (the angular momentum of this state is $-l$ due to the definition $z \equiv x - \imath y$). Then a straightforward calculation[27] yields

$$u(z,Z) = \sum_{l=0}^{\infty} C_l(Z)\psi_l(z), \tag{4}$$

with $C_l(Z) = (Z^*)^l \exp(-ZZ^*/2)/\sqrt{l!}$ for $Z \neq 0$. Naturally, $C_0(0) = 1$ and $C_{l>0}(0) = 0$.

Since electrons in strong magnetic fields are fully polarized, only the space part of the many-body wave functions needs to be considered.[28] The symmetry-broken UHF determinant, $\Psi^N_{\rm UHF}$, describing the WM is constructed out of the localized wave functions $u(z,Z_j^q)$. Using Eq. (4) one finds the following expansion (within a proportionality constant):

$$\Psi^N_{\rm UHF} = \sum_{l_1=0,\ldots,l_N=0}^{\infty} \frac{C_{l_1}(Z_1)C_{l_2}(Z_2),\ldots,C_{l_N}(Z_N)}{\sqrt{l_1!l_2!\cdots l_N!}} \times D(l_1,l_2,\ldots,l_N)\exp\left(-\sum_{i=1}^{N} z_i z_i^*/2\right), \tag{5}$$

where $D(l_1,l_2,\ldots,l_N) \equiv \det[z_1^{l_1}, z_2^{l_2}, \cdots, z_N^{l_N}]$. The Z_k's (with $1 \leqslant k \leqslant N$) in Eq. (5) are the Z_j^q's of Eq. (2), but relabeled.

The UHF determinant $\Psi^N_{\rm UHF}$ breaks the rotational symmetry and thus it is is not an eigenstate of the total angular momentum $\hbar\hat{L} = \hbar\Sigma_{i=1}^N \hat{l}_i$. However, one can *restore*[19,21] the rotational symmetry by applying onto $\Psi^N_{\rm UHF}$ the projection operator[29]

$$\mathcal{O}_L \equiv \prod_{q=1}^{r} \mathcal{P}_{L_q}, \tag{6}$$

with

$$2\pi\mathcal{P}_{L_q} \equiv \int_0^{2\pi} d\gamma_q \exp[\imath\gamma_q(\hat{L}_q - L_q)], \tag{7}$$

where $\hbar\hat{L}_q = \hbar\Sigma_{i=i_q+1}^{i_q+n_q}\hat{l}_i$ and $\hbar L_q = \hbar\Sigma_{i=i_q+1}^{i_q+n_q} l_i$ with $i_q = \Sigma_{s=1}^{q-1} n_s$ $(i_1 = 0)$ are partial angular momenta operators and values, respectively, associated with the qth ring, and $\hbar L = \hbar\Sigma_{q=1}^r L_q$ are the eigenvalues of the total angular momentum.

When applied onto $\Psi^N_{\rm UHF}$, the projection operator $\mathcal{O}_L$ acts as a product of Kronecker deltas: from unrestricted sum (5), it picks up only those terms having a given total angular momentum L and a specific ordered partition of it into partial angular momenta associated with the concentric rings, i.e., $\hbar L = \hbar\Sigma_{q=1}^r L_q$. The final analytic expression depends on the specific ring arrangement $(n_1,n_2,\ldots,n_r)$. For lack of space, we will present here explicitly only the simplest nontrivial arrangement, i.e., (n_1,n_2), with more complex [or simpler ones, i.e., (0,N) and $(1,N-1)$] obtained via straightforward extensions.

For specific electron locations [Eq. (2)] associated with the (n_1,n_2) WM, one derives[30] the following symmetry-preserving, many-body correlated wave functions (within a proportionality constant)

$$\Phi_{L_1,L_2}(n_1,n_2;[z]) = \sum_{0 \leqslant l_1 < l_2 < \cdots < l_N}^{l_1+\cdots+l_{n_1}=L_1, l_{n_1+1}+\cdots+l_N=L_2} \left(\prod_{i=1}^{N} l_i!\right)^{-1} \times \left(\prod_{1 \leqslant i < j \leqslant n_1} \sin\left[\frac{\pi}{n_1}(l_i - l_j)\right]\right) \times \left(\prod_{n_1+1 \leqslant i < j \leqslant N} \sin\left[\frac{\pi}{n_2}(l_i - l_j)\right]\right) D(l_1,l_2,\ldots,l_N) \times \exp\left(-\sum_{i=1}^{N} z_i z_i^*/2\right). \tag{8}$$

In deriving Eq. (8), we took into account that for each determinant $D(l_1,l_2,\ldots,l_N)$ in the unrestricted expansion (5) there are $N!-1$ other determinants generated from it through a permutation of the indices $\{l_1,l_2,\ldots,l_N\}$; these determinants are equal to the original one or differ from it by a sign only.

Generalizations of expression (8) to structures with a larger number r of rings involve, for each additional qth ring $(2 < q \leqslant r)$, (I) the inclusion of an additional product of sines with arguments containing n_q, and (II) a restriction on the summation of the associated n_q angular momenta.

III. PROPERTIES OF THE REM WAVE FUNCTIONS

We call the correlated wave functions [Eq. (8)] the REM wave functions. Among the properties of the REM functions, we mention the following.

(1) The REM wave functions lie entirely within the Hilbert subspace spanned by the lowest Landau level and, after expanding the determinants,[30] they can be written in the form (within a proportionality constant)

$$\Phi_L^N[z] = P_L^N[z]\exp\left(-\sum_{i=1}^{N} z_i z_i^*/2\right), \tag{9}$$

where the $P_L^N[z]$'s are order-L homogeneous polynomials of the z_i's.

(2) The polynomials $P_L^N[z]$ are divisible by

$$P_V^N[z] = \prod_{1 \leqslant i < j \leqslant N} (z_i - z_j), \tag{10}$$

TABLE I. The $Q_9^3[z]$ polynomial associated with the REM and the JL functions (the $Q_L^N[z]$ polynomials are of order $L-L_0$).

REM	$(z_1^3-3z_1^2z_2+z_2^3+6z_1z_2z_3-3z_2^2z_3-3z_1z_3^2+z_3^3)$ $\times(z_1^3-3z_1z_2^2+z_2^3+6z_1z_2z_3-3z_1^2z_3-3z_2z_3^2+z_3^3)$
JL	$(z_1-z_2)^2(z_1-z_3)^2(z_2-z_3)^2$

namely, $P_L^N[z]=P_V^N[z]Q_L^N[z]$. This is a consequence of the antisymmetry of $\Phi_L^N[z]$. $P_V^N[z]$ is the Vandermonde determinant $D(0,1,\ldots,N)$. For the case of the lowest allowed angular momentum $L_0=N(N-1)/2$ (see below), one has $P_{L_0}^N[z]=P_V^N[z]$, a property that is shared with the Jastrow-Laughlin[2] and composite-fermion[3] trial wave functions.

(3) The $P_L^N[z]$'s are translationally invariant functions.

(4) The coefficients of the determinants [i.e., products of sine functions; see Eq. (8)] dictate that the REM functions are nonzero only for special values of the total angular momentum L given for a $(n_1,n_2,\ldots,n_r)$ configuration by

$$L=N(N-1)/2+\sum_{q=1}^{r} n_q k_q, \quad k_q=0,1,2,3,\ldots \tag{11}$$

The minimum angular momentum $L_0=N(N-1)/2$ is determined by the fact that the D determinants [see Eq. (8)] vanish if any two of the single-particle angular momenta l_i and l_j are equal. For the $(0,N)$ and $(1,N-1)$ rings, the special values are given by $L=L_0+Nk$ and $L=L_0+(N-1)k$, respectively. In plots of the energy vs the angular momenta, derived from exact-diagonalization studies,[9–11] it has been found that the special L values associated with the $(0,N)$ and $(1,N-1)$ rings (appropriate for $N\leqslant 7$) exhibit prominent cusps reflecting enhanced stability; as a result these L values are often referred to as "magic angular momenta."[31] We predict that similar magic behavior reflecting enhanced stability is exhibited by the special L values given by Eq. (11) and associated with the general ring arrangement $(n_1,n_2,\ldots,n_r)$. In the thermodynamic limit,[2,5] the total L is related to a fractional filling $\nu=N(N-1)/(2L)$, and thus the angular momenta (11) of the REM functions correspond to all the ν associated with the FQH effect, including the even-denominator ones, i.e., $\nu=1,3/5,3/7,5/7,2/3,1/2,1/3$, etc. . . . .

(5) For the case of two electrons $(N=2)$, the REM functions reduce to the Jastrow-Laughlin form, namely,

$$P_L^2[z]=\prod_{1\leqslant i<j\leqslant N}(z_i-z_j)^L \tag{12}$$

where $L=1,3,5,\ldots$. However, this is the only case for which there is coincidence between the REM and the JL wave functions. For higher numbers of electrons, N, the polynomials $P_L^N[z]$ of the REM functions (apart from the lowest-order Vandermonde $P_{L_0}^N[z]$ ones) are quite different from the corresponding JL or composite-fermion polynomials. In particular, the familiar factor $\Pi_{1\leqslant i<j\leqslant N}(z_i-z_j)^{2p}$, with p an integer[3,4] (which reflects multiple zeroes) does not appear in the REM functions (see, e.g., Table I which contrasts the $Q_9^3[z]$ polynomials corresponding to the REM and JL functions).

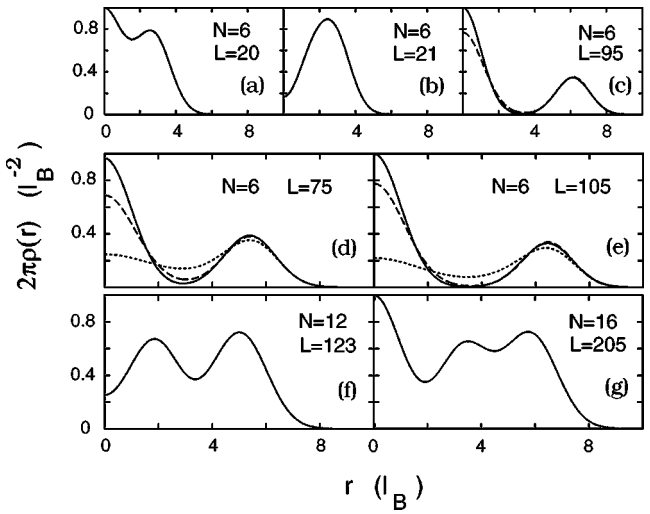

FIG. 1. Radial ED's from REM wave functions (solid lines, all frames), exact diagonalization [dashed lines (a)–(e)], and JL functions [dotted lines (d) and (e)]. In (a) and (b), the solid and dashed curves are practically indistinguishable.

(6) For the case of three electrons $(N=3)$, after transforming to the Jacobi coordinates $\overline{z}=(z_1+z_2+z_3)/3, z_a=(2/3)^{1/2}[(z_1+z_2)/2-z_3], z_b=(z_1-z_2)/\sqrt{2}$ (and dropping the center-of-mass exponential factor), the REM wave functions can be written as (again within a proportionality constant)

$$\Phi_L^3[z_a,z_b]=[(z_a+\imath z_b)^L-(z_a-\imath z_b)^L] \times\exp[(-1/2)(z_a z_a^*+z_b z_b^*)], \tag{13}$$

with $L=3m, m=1,2,3,4,\ldots$, being the total angular momentum. Again the wave functions $\Phi_L^3[z_a,z_b]$ are very different from the three-electron JL ones; e.g., they are nonvanishing for even m values, unlike the three-electron JL functions. However, the $\Phi_L^3[z_a,z_b]$'s coincide with the functions $|m,0\rangle$ derived in Ref. 1. We remark that, although it was found[1] that these wave functions exhibited a behavior expected of fractional quantum Hall ground states (e.g., areal quantization and incompressibility), the generalization of them to a higher number of electrons did not follow; instead, the REM functions presented here do constitute such a generalization.

IV. OSCILLATORY ELECTRON DENSITIES

In Fig. 1, we display the radial ED's of several REM wave functions and compare them to corresponding ED's from exact diagonalizations. The main conclusion is that the ED's of the REM functions exhibit[32] a prominent oscillatory behavior in excellent agreement with the exact ED's. Such an oscillatory behavior is a natural consequence of the underlying ring arrangements. For $N=6$ and $L=20$, the underlying structure is a (1,5) arrangement [L is five units larger than the minimum $L_0=15$, i.e., $n_1=1, k_1=0$ and n_2

$=5,k_2=1$ in Eq. (11)], and thus the corresponding ED exhibits a maximum at the origin followed by an outer hump [Fig. 1(a)]. For $N=6$ and $L=21$, however, the underlying structure is a (0,6) arrangement (L is six units larger than L_0), and thus the ED exhibits a dip at the origin and a single outer hump [Fig. 1(b)]. In the other $N=6$ cases plotted here [Figs. 1(c), 1(d), and 1(e)], the difference $L-L_0$ is divisible by 5 and the underlying ring arrangement is (1,5); thus there are two humps in the corresponding ED's, the inner one portraying the single electron at the origin. The $N=6,L=75$ [Fig. 1(d)] and $N=6,L=105$ [Fig. 1(e)] cases correspond to the fractional fillings 1/5 and 1/7, respectively. For these two cases, we have plotted also the ED's associated with the JL functions (dotted lines). As was found in the $\nu=1/3$ case,[18] the JL functions fail to capture the radial oscillations that are characteristic of the long-range Coulomb force. Finally, in Fig. 1(f) and Fig. 1(g), we present the ED's of the REM functions for $N=12,L=123$ and $N=16,L=205$. In general, there are as many humps as the number of concentric rings. Indeed the ring structures are[12,25] (3,9) and (1,5,10) for $N=12$ and $N=16$, respectively.[33] We note that the ED for $N=12,L=123$ is similar to the exact ED for the same case,[34] although the latter was calculated with an external confinement.

It has been found[12,25] that the number of rings (r) increases as the number of electrons grows. For $\nu\leqslant 1/3$, this results in electron-density oscillations that extend along the whole radius of the QD, with no obvious separation into bulk and edge regions. Currently, the largest number of electrons for which the ring structure has been determined[25] is $N=230$ with a concentric-ring arrangement of (1,6,12,18,23,25,34,37,37,37).

V. CONCLUSIONS

We have developed a class of trial wave functions of simple functional form, which accurately describe the physics of electrons in QD's under high magnetic fields. In particular, our functions capture the long-range correlations of the Coulomb repulsion; unlike the JL functions, they yield for all N and fractional fillings ν an oscillatory radial electron density in agreement with exact-diagonalization results. The electron-density oscillations extend throughout the system. The thematic basis of our approach is built upon the intuitive, but *microscopically* supported, picture of collectively rotating electron molecules, and the synthesis of the many-body REM wave functions involves breaking of the circular symmetry at the UHF level with subsequent restoration of this symmetry via a projection technique. While we focus here on the strong magnetic-field regime, we note that the REM picture unifies the treatment of strongly correlated states of electrons in QD's over the whole magnetic-field range.[13,20,21,24] Finally, our REM wave functions, aimed here mainly at treating finite electron systems (i.e., QD's), can provide in the thermodynamic limit an alternative interpretation of the FQH effect; namely, the observed hierarchy of fractional filling factors may be viewed as a signature originating from the magic angular momenta of rotating electron molecules.

ACKNOWLEDGMENT

This research was supported by the U.S. D.O.E. (Grant No. FG05-86ER-45234).

[1] R.B. Laughlin, Phys. Rev. B **27**, 3383 (1983).
[2] R.B. Laughlin, Phys. Rev. Lett. **50**, 1395 (1983).
[3] J.K. Jain, Phys. Rev. B **41**, 7653 (1990).
[4] J.K. Jain and T. Kawamura, Europhys. Lett. **29**, 321 (1995).
[5] S.M. Girvin and T. Jach, Phys. Rev. B **28**, 4506 (1983).
[6] L. Jacak, P. Hawrylak, and A. Wojs, *Quantum Dots* (Springer, Berlin, 1998), and references therein.
[7] A. Wojs and P. Hawrylak, Phys. Rev. B **56**, 13227 (1997).
[8] S.-R. Eric Yang, A.H. MacDonald, and M.D. Johnson, Phys. Rev. Lett. **71**, 3194 (1993).
[9] W.Y. Ruan, Y.Y. Liu, C.G. Bao, and Z.Q. Zhang, Phys. Rev. B **51**, 7942 (1995).
[10] T. Seki, Y. Kuramoto, and T. Nishino, J. Phys. Soc. Jpn. **65**, 3945 (1996).
[11] P.A. Maksym, H. Imamura, G.P. Mallon, and H. Aoki, J. Phys.: Condens. Matter **12**, R299 (2000), and references therein.
[12] H.-M. Müller and S.E. Koonin, Phys. Rev. B **54**, 14532 (1996).
[13] C. Yannouleas and U. Landman, Phys. Rev. B **61**, 15895 (2000).
[14] C. Yannouleas and U. Landman, Int. J. Quantum Chem. **90**, 699 (2002).
[15] F.D.M. Haldane, Phys. Rev. Lett. **51**, 605 (1983); S.A. Trugman and S. Kivelson, Phys. Rev. B **31**, 5280 (1985).
[16] A.M. Chang, M.K. Wu, C.C. Chi, L.N. Pfeiffer, and K.W. West, Phys. Rev. Lett. **86**, 143 (2001), and references therein.
[17] V.J. Goldman and E.V. Tsiper, Phys. Rev. Lett. **86**, 5841 (2001).
[18] E.V. Tsiper and V.J. Goldman, Phys. Rev. B **64**, 165311 (2001).
[19] P. Ring and P. Schuck, *The Nuclear Many-body Problem* (Springer, New York, 1980), Chap. 11, and references therein.
[20] C. Yannouleas and U. Landman, Phys. Rev. Lett. **82**, 5325 (1999); **85**, 2220(E) (2000).
[21] C. Yannouleas and U. Landman, J. Phys.: Condens. Matter **14**, L591 (2002).
[22] K. Maki and X. Zotos, Phys. Rev. B **28**, 4349 (1983).
[23] Depending on the strength of the interelectron repulsion, WM's can also form at zero magnetic field; see Refs. 13, 20, and 21. For a CPD/exact-solution study of such WM's at $B=0$, see Ref. 24.
[24] C. Yannouleas and U. Landman, Phys. Rev. Lett. **85**, 1726 (2000).
[25] V.M. Bedanov and F.M. Peeters, Phys. Rev. B **49**, 2667 (1994).
[26] A certain degree of Wigner crystallization has also been found in another geometry, i.e., in an infinite Hall bar at an integral filling factor $\nu=2$; see J.P. Rodriguez, M.J. Franco, and L. Brey, Phys. Rev. B **61**, 16787 (2000).
[27] S.A. Mikhailov, Physica B **299**, 6 (2001).
[28] In our earlier publications (Refs. 13, 14, 20, and 21), we have used the term spin-and-space (sS)-UHF to emphasize the break-

ing of both the spin and space symmetries. In this paper, only the breaking of the space symmetry is involved.

[29] Projection operator (6) is a generalization of the simpler $\mathcal{P}_L$ operator used for restoring the circular symmetry in the simplest (0,N) and (1,N-1) ring arrangements (Ref. 21), or for objects without a ring structure (Ref. 19).

[30] The algebraic manipulations reported here were performed using MATHEMATICA; see S. Wolfram, *Mathematica: A System for Doing Mathematics by Computer* (Addison-Wesley, Reading, MA, 1991).

[31] The magic angular momenta for $N \leqslant 7$ have been also discussed in the context of the geometric configuration (Refs. 9 and 10) and the Eckart frame (Ref. 11) models. However, unlike our approach, these models do not afford derivation of analytical forms for the REM wave functions.

[32] The REM functions also have close-to-unity overlaps with the exact wave functions. For an example, see Table II in ArXiv: cond-mat/0202062 (unpublished).

[33] In Eq. (11), the corresponding k_q values are $k_1=1, k_2=6$; $k_1=0$, $k_2=3$, and $k_3=7$.

[34] See Fig. 3(f) in X. Wan, K. Yang, and E.H. Rezayi, Phys. Rev. Lett. **88**, 056802 (2002).